Refined structure of melittin bound to perdeuterated dodecylphosphocholine micelles as studied by 2D-NMR and distance geometry calculation. Proteins 9:81-89

ARTICLE *in* PROTEINS STRUCTURE FUNCTION AND BIOINFORMATICS · FEBRUARY 1991

Impact Factor: 2.63 · DOI: 10.1002/prot.340090202 · Source: PubMed

3 AUTHORS, INCLUDING:

Nobuhiro Go
Japan Atomic Energy Agency
238 PUBLICATIONS **10,099** CITATIONS
SEE PROFILE

Fuyuhiko Inagaki
Hokkaido University
326 PUBLICATIONS **8,952** CITATIONS
SEE PROFILE

PROTEINS: Structure, Function, and Genetics 9:81–89 (1991)

Research Articles

Refined Structure of Melittin Bound to Perdeuterated Dodecylphosphocholine Micelles as Studied by 2D-NMR and Distance Geometry Calculation

Teikichi Ikura,[1] Nobuhiro Gō,[1] and Fuyuhiko Inagaki[2]

[1]Department of Chemistry, Faculty of Science, Kyoto University, Sakyo-ku, Kyoto 606, Japan; and [2]Department of Molecular Physiology, The Tokyo Metropolitan Institute of Medical Science, 3-18-22, Honkomagome, Bunkyo-ku, Tokyo 113, Japan

ABSTRACT **In our previous paper we reported the conformation of melittin bound to perdeuterated dodecylphosphocholine micelles as studied by ^{1}H NMR experiment and distance geometry calculation. No hydrogen bonds were taken into consideration explicitly in the calculation. However, mostly α-helical conformations were obtained as results of the calculation even with no explicitly assumed hydrogen bonds. In the present paper we refined the distance geometry calculation by incorporating hydrogen bonds suggested by the previous calculation. As a result, we obtained the conformation of melittin, which was consistent with both NMR data and the additional hydrogen bonding data. The α-helical rod in the refined conformation also has a kink at Thr-11 and Gly-12, but its bent angle is now a bit narrowly distributed in 135° ± 15°. In the present study another distortion at Trp-19 and Ile-20 becomes conspicuous. The average root-mean-square displacement of atoms is now much smaller and is 1.5 Å for all backbone atoms. In the present paper side chain conformations are also analyzed.**

Key words: 2D-NMR experiment, distance geometry, hydrogen bond, side chain conformation

INTRODUCTION

Melittin is a small single-chain polypeptide containing 26 amino acids,[1,2] and is included in the venom of the honey bee. Since melittin has a strong hemolytic activity, it is important to determine its conformation and to elucidate its interaction with membrane. For this purpose, many studies have been pursued by using various methods.[3–7] Particularly, determination of the conformation of melittin as bound to micelles is expected to be useful for guessing its conformation bound to membrane. In that respect, Brown et al. in a pioneering work used the NMR experiment. It is generally difficult to eliminate the huge proton resonances from micelles and the spin diffusion effects on NMR study in micelles. However, these problems were overcome by the use of the perdeuterated micelles.[8,9] Thus, we studied the conformation of melittin bound to micelles by using 2D-NMR and distance geometry calculation, and reported its result in our previous paper.[10]

In our previous calculation hydrogen bonds were not taken into consideration explicitly. However, mostly α-helical conformations were obtained as a result of the calculation even with no explicitly assumed hydrogen bonds. This means that the body of the NMR data strongly indicates the α-helical conformation. In the present paper we refined the distance geometry calculation by using additional information about hydrogen bonds suggested by the previous calculation. As a result, we obtained the conformation of melittin which was consistent with both NMR data and the additional hydrogen bonding data.

MATERIAL AND METHODS

Calculation

The distance geometry calculation was done by using the program DADAS (distance analysis in dihedral angle space),[11] in which bond lengths, bond angles, and peptide bond dihedral angles are fixed at ECEPP (empirical conformational energy program for peptides) values[12,13] and the remaining dihedral angles are treated as independent variables. The distance constraints were obtained from the NOESY spectra of NMR experiment. Since stereospecific resonance assignments could not be done for the indi-

Received August 30, 1989; revision accepted August 22, 1990.

Address reprint requests to Nobuhiro Gō, Department of Chemistry, Faculty of Science, Kyoto University, Sakyo-ku, Kyoto 606, Japan.

vidual protons in methylene groups or methyl groups, pseudo-atom representations were used where appropriate. All calculations were carried out with FACOM M780 and HITAC M680H computers at Computer Centers, Kyoto University and Institute for Molecular Science, respectively. Molecular drawing were carried out with the CHARMm/QUANTA program on the IRIS-4D/70G computer at Tokyo Metropolitan Institute of Medical Science.

Analysis of Side Chain

We also analyzed the side chain conformations in the obtained conformations. If a χ angle in each obtained conformation was distributed within a range of about 30°, we considered it as staying within one potential minimum for the side chain.

RESULTS

Experimental Distance Constraints

The NOESY cross-peaks were recorded with mixing times of 80 and 150 ms. Assignments of these cross-peaks were made based on the previously obtained complete set of sequence-specific resonance assignments. Upper bound distance constraints for distance geometry calculation were derived from the crude calibration that NOESY cross-peak intensity is proportional to the inverse of the sixth power of the distance. NOESY cross-peaks were divided into four categories: strong, medium-strong, medium, and weak. Upper bound constraints of 2.5, 3.0, 3.5, and 4.0 Å are assumed, respectively. These calibrations were used for the intraresidue and sequential NOESY cross-peaks. For the long-range NOESY cross-peaks, a fixed upper bound constraint of 5.0 Å was adopted. Where appropriate, pseudo-atom correction factors were added to the upper bound constraints. Numbers of upper bound constraints derived from NOESY spectra were 68, 52, and 119 for intraresidue, sequential, and long-range constraints, respectively. Figure 1 shows the survey of the sequential and long-range distance constraints used in the present calculation.

Hydrogen Bonds

The previous result indicated that the conformation of melittin is mostly α-helical. However, the calculated α-helical conformations are distorted slightly because of our calculation with no explicitly assumed hydrogen bonds. In order to eliminate this distortion we prepared a list of hydrogen bonds which are positively indicated from the α-helical conformations and added this information in the refined distance geometry calculation. The preparation of the list is done iteratively as follows.

At first we obtained five "good" conformations with a relatively small number of residual violations (the violations of the distance constraints for NOEs were smaller than 0.3 Å) by the previous distance geometry calculations with *no explicitly assumed hydrogen bonds*. Each of these five conformations was closely examined by computer graphics to see if hydrogen bonds could be formed. Only cases where local conformations clearly ruled out formation of hydrogen bonds were judged as no hydrogen bond formed, i.e., in ambiguous cases hydrogen bonds were assumed as formed. At this stage, a hydrogen bond was judged as formed, when it was judged as formed in at least one of the five conformations. Thus we obtained a "loose" list of hydrogen bonds. At the next step, hydrogen bonds in this list were treated as formed and the distance geometry calculations were carried out to examine if the standard hydrogen bond geometry (distance between the amide hydrogen and the carbonyl oxygen is between 2.0 and 1.8 Å, and the distance between the amide nitrogen and the carbonyl oxygen is between 3.0 and 2.7 Å) and local NOE distance constraints were satisfied simultaneously. A few hydrogen bonds were found unsatisfactory. Then, these hydrogen bonds were eliminated from the list. The distance geometry calculations were repeated a few times in this manner until no further unsatisfactory hydrogen bonds were observed. The hydrogen bonding pairs which remained in the final list were 2O-6H^N, 3O-7H^N, 4O-8H^N, 5O-9H^N, 6O-10H^N, 7O-10H^N, 8O-12H^N, 12O-16H^N, 13O-17H^N, 14O-18H^N, 17O-21H^N, 20O-24H^N, 21O-25H^N, and 22O-26H^N. All of them but 7O-10H^N, which is an i to $i+3$ hydrogen bond, are standard i to $i+4$ α-helical hydrogen bonds.

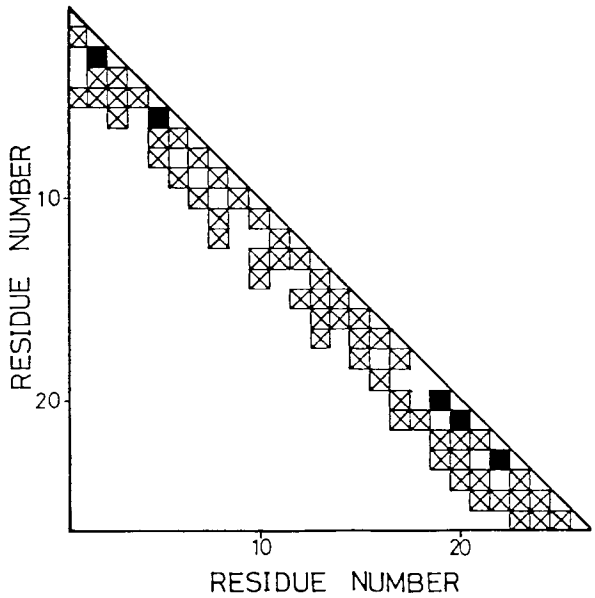

Fig. 1. Survey of sequential and long-range NOE-derived distance constraints for melittin bound to the DPC micelles. Both axes pertain to the sequence of melittin. Crossed squares indicate that the number of NOE constraints is from 1 to 5. Filled squares from 6 to 10. There are no NOE constraints between amino acid residues with more than five residues apart. The NOE constraints were derived from 80 and 150 ms NOESY spectra.

TABLE I. Statistics of Violations of the Residual Distance Constraints in the Conformations of Melittin Computed From the NOE and Hydrogen Bonding Data Using DADAS

	Sum of violations(Å)		Numbers of violations in distance Constraints (Å)		Numbers of violations in steric constraints
			NOE	H-bond	
Conformation	NOE	H-bond	(>0.1 Å)	(>0.05 Å)	(>0.1 Å)
1	0.82	0.43	2 (0.10)*	3 (0.10)	1 (0.29)
2	0.87	0.28	3 (0.23)	2 (0.06)	1 (0.24)
3	0.90	0.19	2 (0.23)	0 (0.04)	2 (0.29)
4	1.25	0.45	5 (0.27)	2 (0.14)	1 (0.31)
5	1.35	0.51	3 (0.24)	3 (0.07)	0 (0.08)

*The largest violations are given in parentheses.

Distance Geometry Calculation

Starting conformations were generated as follows. First, many conformations were generated from randomly selected dihedral angles. Second, distance geometry calculation without the van der Waals term for intraresidue and sequential NOE distance constraints had been carried out for them. If a conformation had no distance constraint violation larger than 0.1 Å, it was selected as a starting conformation. After all, we had 100 starting conformations. The RMSDs for the backbone atoms calculated for all pairs of starting conformations were 10.1 ± 5.1 Å. These values indicate that the generated conformations were random enough.

After a number of distance geometry calculations, the five conformations which best satisfied the experimental distance constraints were selected for further study and comparison.

Table I shows the residual violations of the distance constraints. The largest violations of the distance constraints for NOEs and hydrogen bonds in the five conformations were 0.10~0.27 and 0.04~0.14 Å, respectively. The steric violations larger than 0.3 Å were not observed except in one conformation (conformation #4). The sums of violations of the distance constraints for NOEs and hydrogen bonds in the five conformations were 0.82~1.35 and 0.19~0.51 Å, respectively. Figure 2 shows the superposition of the five backbone conformations. The RMSDs for the backbone atoms for each pair of the five conformations were calculated (Table II). The average RMSD for the whole residue of them was 1.5 Å (Fig. 2a). For two segments of Gly-1–Thr-10 and Leu-13–Gln-26, the average RMSD was 0.5 and 1.0 Å, respectively (Fig. 2b,c).

Side Chain Conformations

We analyzed the distribution of χ angles of each residue in the five conformations. The following side chain χ angles were found to be distributed in a single potential minimum: $\chi 2$ of Ile-2, $\chi 1$ and $\chi 3$ of Val-5, $\chi 1$ and $\chi 2$ of Val-8, $\chi 3$ of Thr-11, $\chi 1$ of Ala-15, $\chi 1$ of Leu-16, $\chi 1$ and $\chi 2$ of Trp-19, $\chi 1$, $\chi 2$, and $\chi 4$ of Ile-20, $\chi 1$, $\chi 2$, and $\chi 3$ of Lys-23. Figures 3 and 4 show examples of the side chains which are found in a defined configuration.

DISCUSSION

In the present calculation we obtained conformations which are much narrowly distributed in RMSD (see Results and Table II) than the one obtained in the previous calculation (the average RMSD of the individual segments of Gly-1–Thr-10 and Leu-13–Gln-26 for the backbone atoms was 1.7 and 1.3 Å, respectively[10]). However, the two sets of conformations satisfy the NOE distance constraints roughly to the same extent. This means that the range of distribution of conformations in the present calculation is included in the older range of distribution. In this sense the results we obtained in the present calculation are consistent with the previous calculation. The narrower distribution is a result of the added new information about the formation of α-helical hydrogen bonds. This new information is, however, indicated from the NOE constraints used already in the previous calculation. The underlying logic of the distance geometry calculation is that a proper set of NOE distance constraints has a much larger amount of information than each isolated constraint. The iterative use of the distance geometry calculation employed in this paper is now shown to be effective to deduce additional information which such a set can have about hydrogen bonds.

It may be worthwhile to look at the above iterative procedure from a different point of view. Even though a set of the hydrogen bond constraints is added as new one, it was derived from a set of initial experimental distance constraints by the iterative procedure. Therefore, this new added set of constraints contains, in a sense, no new information, but expresses a set of information pertaining to such local structures as formation of individual hydrogen bonds, which, in the initial experimental distance constraints, exists not as localized information but

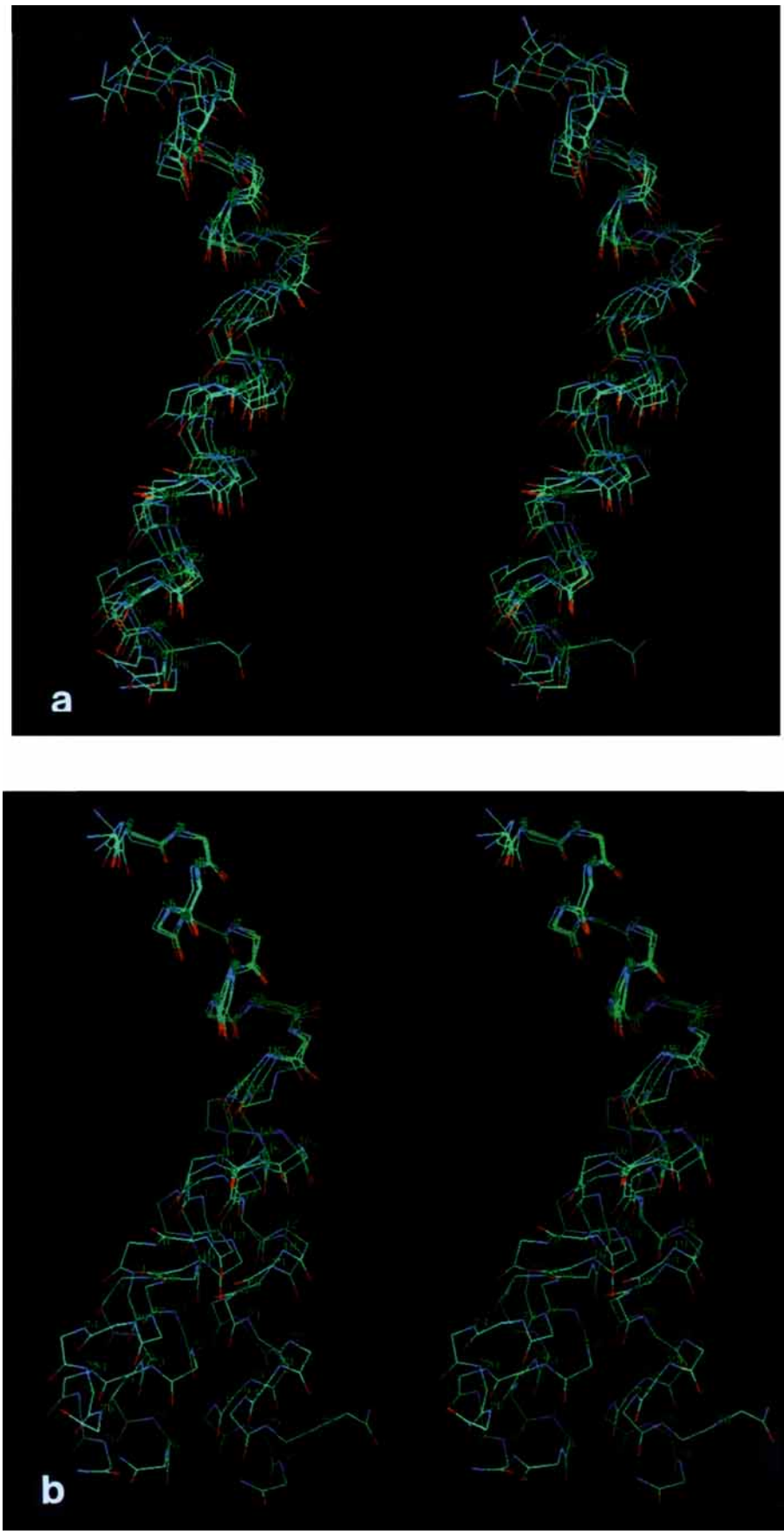

Fig. 2a–b.

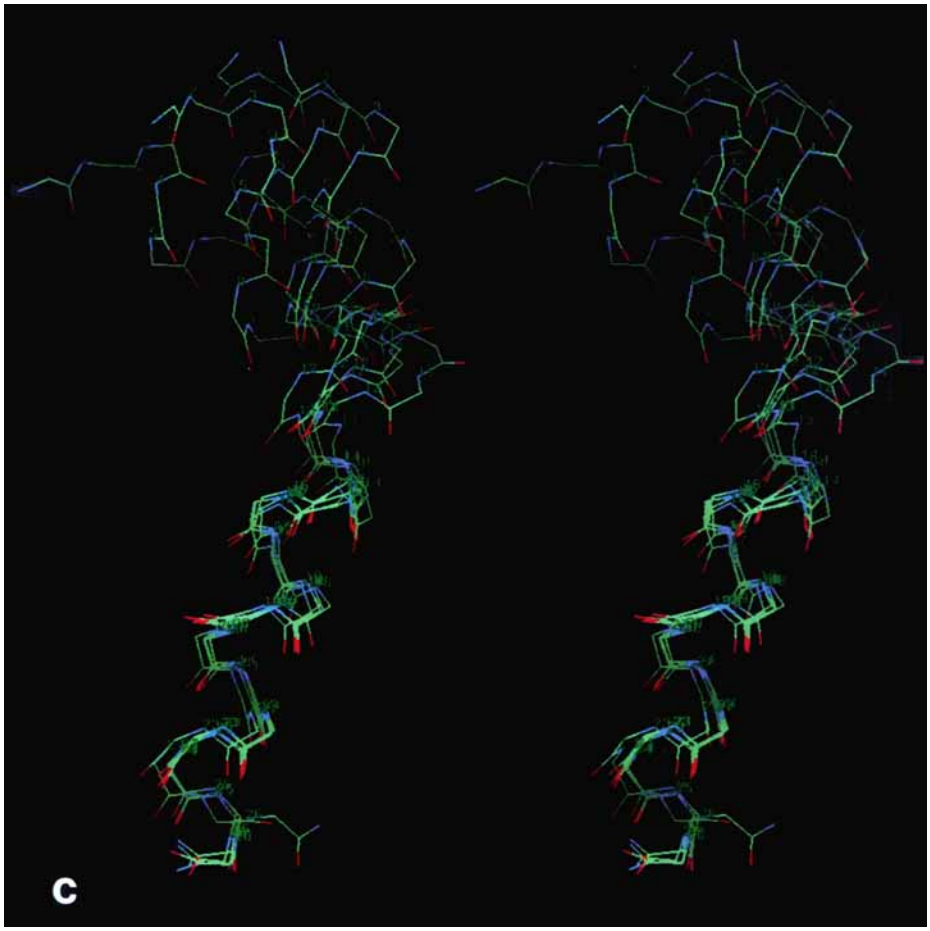

Fig. 2. Stereo view of superposed five conformations of melittin least-square-fitted (**a**) for the whole residue (the average backbone RMSD is 1.5 Å), (**b**) for a segment of Gly-1–Thr-10 (the average RMSD is 0.5 Å), and (**c**) for a segment of Leu-13–Gln-26 (the average RMSD is 1.0 Å). The N, C^{α}, C′, and O atoms are drawn.

TABLE II. The Root-Mean-Square Deviation (RMSD) for Backbone Atoms Between Five Obtained Conformations of Melittin (Å)*

	Conformation			
Conformation	2	3	4	5
1	1.2 (0.5/1.4)	1.6 (0.5/1.4)	2.0 (0.5/1.3)	2.3 (0.4/1.5)
2		0.9 (0.5/0.5)	1.5 (0.4/0.6)	1.8 (0.5/0.8)
3			1.5 (0.5/0.6)	1.3 (0.2/0.7)
4				1.3 (0.5/0.7)

*The RMSDs for segments between Gly-1 and Thr-10 and between Leu-13 and Gln-26 are given on the left and right side in parentheses, respectively.

as information distributed in many constraints. Because we add information which already exists in a distributed form in the initial set of constraints, we do not change the information contained in the target function, but change only relative weights of various different information contained in it. This change of relative weights has been found in this paper to affect the RMSD of conformations obtained by the calculation. In the current methodology of distance geometry calculation a group of conformations which is more-or-less consistent with experimental data is obtained. The RMSD of the conformations thus obtained is then calculated and discussed. However, the current methodology still lacks the firm theoretical foundation to judge how much of the calculated RMSD reflects the dynamic thermal conformational fluctuations. In this situation it is interesting to note that the target functions

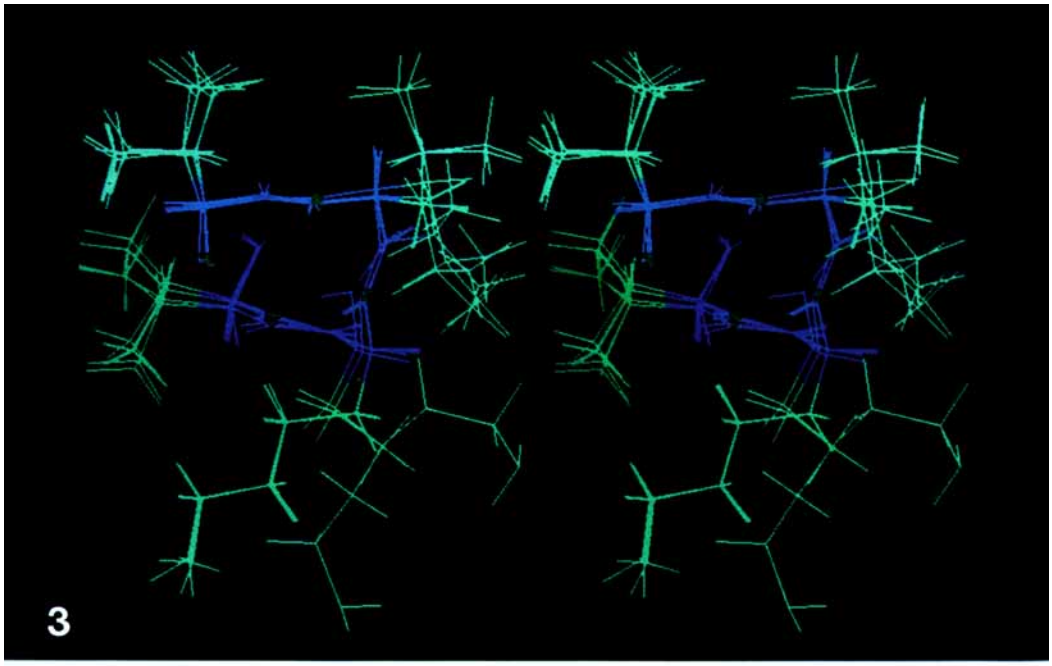

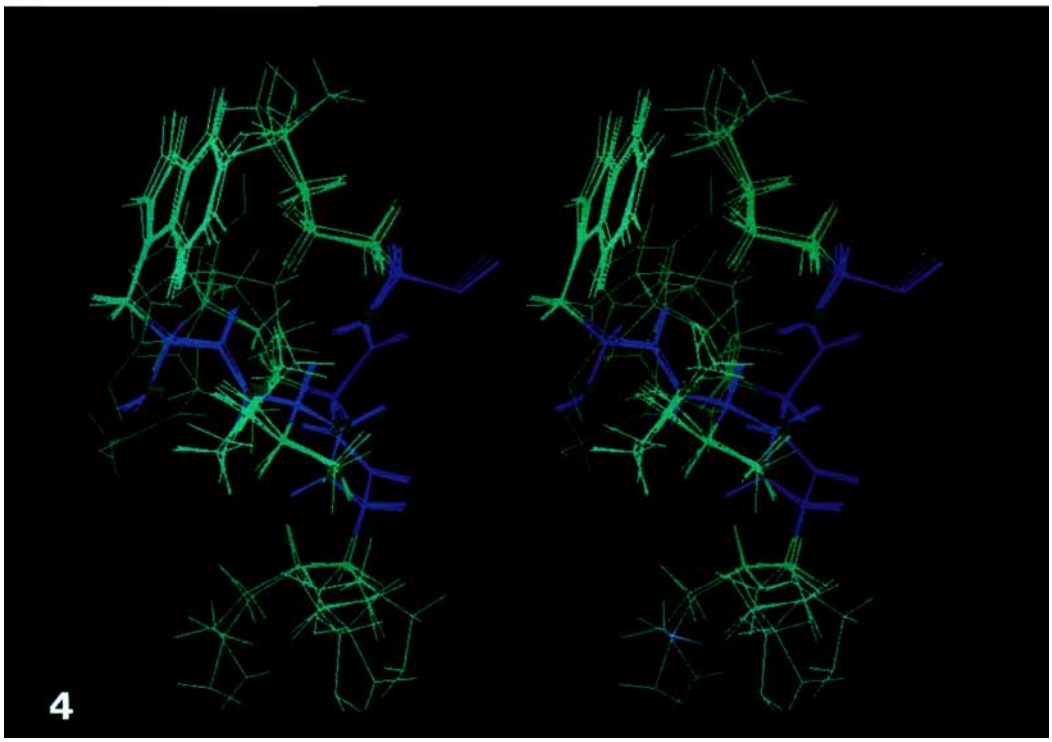

Fig. 3. Stereo view of superposition of a segment from Val-5 to Val-8 in the five conformations of melittin. The side chains of Val-5 and Val-8 are observed in a defined configuration.

Fig. 4. Stereo view of superposition of a segment from Trp-19 to Lys-23 in the five conformations of melittin. The side chains of Trp-19, Ile-20, and Lys-23 are observed in a defined configuration. The side chain of Lys-23 approaches the indole ring of Trp-19.

containing the same information, but with different relative weights, produce conformations with the different RMSD.

The new added constraints for the hydrogen bonds play a similar role with an energy term for hydrogen bond formation. If such an energy term were included in our distance geometry calculation, conformations likely to form a hydrogen bond are stabilized by the energy and will therefore be narrowly distributed. From such a similarity we strongly feel

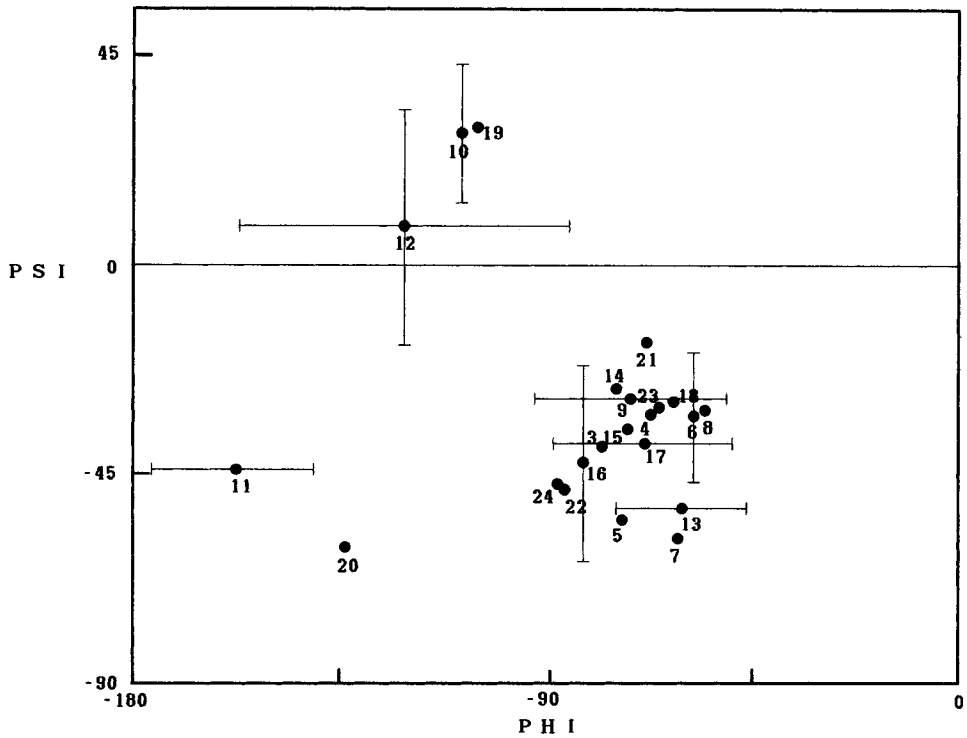

Fig. 5. The Ramachandran plot for melittin. The residue number is written near the average point corresponding to its pair of angles. When an angle is distributed in the range of more than 20°, a bar is given to indicate its maximum and minimum values. When the distribution is within 20°, only the average point is indicated. N- and C-terminal regions, Gly-1, Ile-2, Gln-25, and Gln-26, are not plotted. The ϕ angle of Pro-14 is fixed at $-75.0°$.

that the smaller value of RMSD obtained in this paper as compared with the value obtained in the previous paper reflects the reality.

The conformation obtained by the present calculation is similar to that obtained in the previous one in that it is a rodlike α-helical conformation with a kink at Thr-11 and Gly-12. However, the bent angle is now a bit narrowly distributed, i.e., 135 ± 15° (Fig. 2), while in the previous report it was 120–160°. However, this kink portion is still less well defined than the other portions. This is seen from the distribution of ϕ and ψ angles, i.e., those of Gly-12 are larger than those of the other residues except N and C terminals (Fig. 5).

Figure 5 shows the regions of the standard α-helix of melittin, too. Standard α-helices are observed in the regions from Gly-3 to Leu-9, Leu-13 to Ser-18, and Lys-21 to Arg-24. The non-α-helical values of (ϕ, ψ) of three residues from Thr-10 to Gry-12 corresponded to the kink at Thr-11 and Gly-12. Another distortion of the α-helix is observed at Trp-19 and Ile-20. This distortion is likely caused by an approach of the side chain of Lys-23 to the indole ring of Trp-19 (Fig. 4), which is consistent with the high field shift of H^{γ} of Lys-23 (Table I in our previous report[10]). In the conformation revealed by X-ray crystallographic analysis,[4,5] the kink at Thr-11 and Gly-12 was observed. However, the distortion at Trp-19 and Ile-20, which is observed in this paper, was not observed in the X-ray conformation. Both side chains of Trp-19 and Lys-23 in the NMR revealed the conformation exists on the hydrophobic side of the α-helical rod (Fig. 10 in the previous paper[10]. Therefore, they are expected to be located in the micelle environment. As stated above, they are very close in space (distances between $N^{\epsilon 1}$ of Trp-19 and C^{ϵ} of Lys-23 and between $C^{\delta 1}$ of Trp-19 and C^{ϵ} of Lys-23 are 3.30 and 3.68 Å, respectively). The two side chains are on the same side of the α-helical rod also in the X-ray conformation. However, they are not so close in space as in the NMR conformation (distances between $N^{\epsilon 1}$ of Trp-19 and C^{ϵ} of Lys-23 and between $C^{\delta 1}$ of Trp-19 and C^{ϵ} of Lys-23 are 7.38 and 8.26 Å, respectively). This difference in the proximity of the two side chains, which should be a consequence of the difference of the environments, may be the reason for the main chain distortion observed in the NMR conformation.

The validity of the use of the distance geometry calculation to extract additional conformational information from a set of NOE constraints and to deduce more reliable conformation is supported by the reasonableness of the obtained list of hydrogen bonds. It is known that slowly exchangeable amide protons can be attributed to hydrogen bonds in solution. We observed that the amide protons of Val-5,

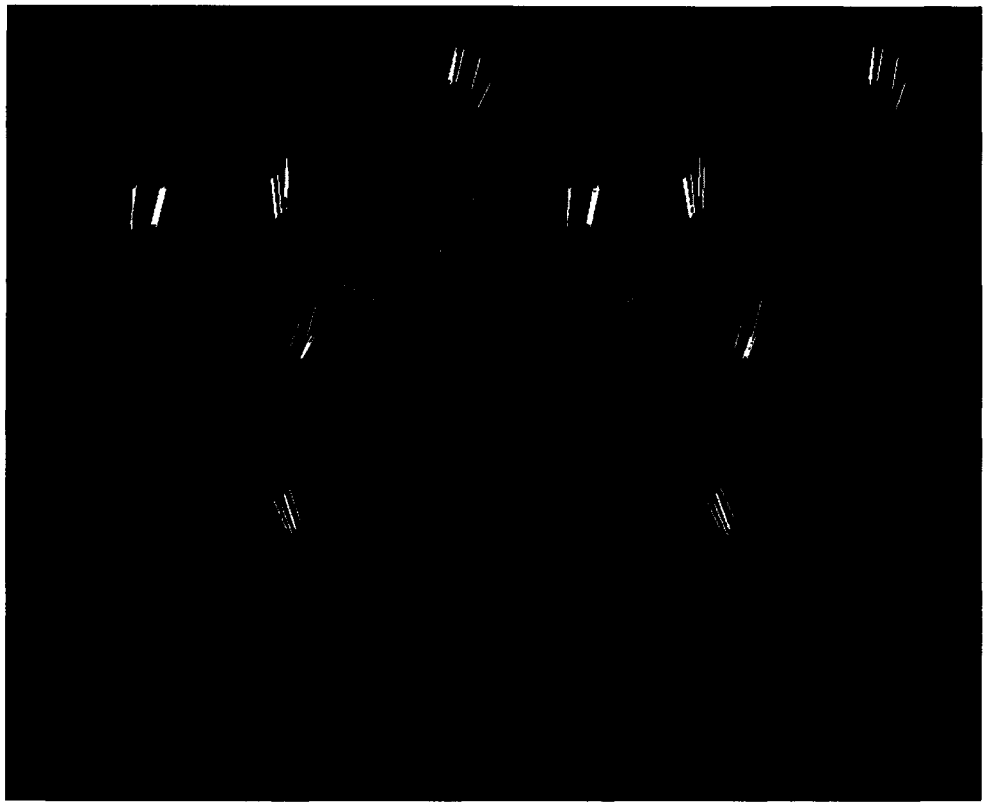

Fig. 6. Stereo view of superposition of a segment from Leu-6 to Thr-10 in the five conformations of melittin. The H^N atom of Thr-10 is seen to be forming a bifurcated hydrogen bond with both 6O and 7O.

Leu-6, Leu-9, Leu-13, Ile-17, Trp-19, Ile-20, Lys-21, and Arg-22 exchanged slowly with solvent.[10] However, we could not regard all slowly exchanging amide protons as due to hydrogen bond formation, because our experiment was done in the micelle environment and amide protons in micelles exchanged slowly with solvent. In this situation, our strategy in this paper is powerful to identify hydrogen bonds. We determined that the slowly exchangeable amide protons of Leu-6, Leu-9, Ile-17, and Lys-21 were due to hydrogen bonds. The rest of the slowly exchangeable amide protons were not attributed to hydrogen bonds, but they were located in the micelles. Most of the other hydrogen bonds identified in this paper were consistent with the NOE patterns of $d_{\alpha N}(i,i+3)$, $d_{\alpha N}(i,i+4)$, and $d_{\alpha\beta}(i,i+3)$ (Fig. 7 in our previous report[10]). The hydrogen bonds were formed almost entirely along this roughly α-helical molecule except at two portions where the helical conformation was distorted either by the presence of the proline residue or by a side chain–side chain interaction. It is interesting that one α-helical hydrogen bond is nonetheless found in each of the two distorted portions, i.e., that between a hydrogen bonding pair 8O-12H^N and that between a pair of 17O-21H^N in the first and the second distorted portions, respectively. Interesting is the finding of a bifurcated hydrogen bond at the C-terminal end of the first α-helix, in which 10H^N is hydrogen bonded to both of 6O and 7O (Fig. 6).

To compare the conformation thus determined by NMR with the X-ray conformation[4,5] hydrogen atoms were added to the X-ray conformation according to the ECEPP standard residue geometry and then the following 16 hydrogen bonds were identified: 2O-6H^N, 3O-7H^N, 4O-8H^N, 5O-9H^N, 6O-10H^N, 8O-12H^N, 13O-17H^N, 14O-18H^N, 15O-19H^N, 16O-20H^N, 17O-21H^N, 18O-22H^N, 19O-23H^N, 20O-24H^N, 21O-25H^N, and 22O-26H^N. Most of them are conserved in the NMR conformation. A few hydrogen bonds are different between the two conformations. They are observed in the two distorted portions, i.e., 7O-10H^N is identified only in the NMR conformation, and 15O-19H^N, 16O-20H^N, 18O-22H^N, and 19O-23H^N are identified only in the X-ray conformation. These differences should be attributed to the difference in the environments, i.e., one in the micelle bound state and the other in crystal.

The power of distance geometry calculation can be seen also in the obtained side chain conformations. It is generally difficult to determine conformations of methylene groups, methyl groups, and aromatic rings by simple interpretations of experimental

NMR data, unless involved hydrogens are stereospecifically assigned. Because they were not assigned stereospecifically, pseudo-atom representations were used in our calculation. However, the methylene side chains of Trp-19 were found in a defined configuration. This illustrates the case where the stereospecific resonance assignment is difficult experimentally but can be made from the calculated conformation.

ACKNOWLEDGMENTS

Computations were done at Computer Centers of Kyoto University and of Institute for Molecular Science. This work has been supported by Kyoto University by grants to Nobuhiro Gō from MESC and STA.

REFERENCES

1. Habermann, E. Bee and wasp venoms. Science 177:314–322, 1972.
2. Habermann, E., Jentsch, J. Sequenzanalyse des melittins aus den tryptischen und peptischen spaltstucken. Hoppe Seyler's Z. Physiol. Chem. 348:37–50, 1967.
3. Knöppel, E., Eisenberg, D., Wickner, W. Interactions of melittin, a preprotein model, with detergents. Biochemistry 18:4177–4181, 1979.
4. Terwilliger, T. C., Eisenberg, D. The structure of melittin: II. interpretation of the structure. J. Biol. Chem. 257: 6016–6022, 1982.
5. Terwilliger, T. C., Eisenberg, D. The structure of melittin in the form I crystals and its implication for melittin's lytic and surface activities. Biophys. J. 37:353–361, 1982.
6. Bernheimer, A. W., Rudy, B. Interactions between membranes and cytolytic peptides. Biochim. Biophys. Acta 864: 123–141, 1986.
7. Bazzo, R., Tappin, M. J., Postore, A., Harvey, T. S., Carver, J. A., Campbell, I. D. The structure of melittin: A ^{1}H-NMR study in methanol. Eur. J. Biochem. 173:139–146, 1988.
8. Brown, L. R., Wüthrich, K. Melittin bound to dodecylphosphocholine micelles: ^{1}H-NMR assignments and global conformational features. Biochim. Biophys. Acta 647:95–111, 1981.
9. Brown, L. R., Kumar, A., Wüthrich, K. High resolution nuclear magnetic resonance studies of the conformation and orientation of melittin bound to lipid-water interface. Biophys. J. 37:319–328, 1982.
10. Inagaki, F., Shimada, I., Kawaguchi, K., Hirano, M., Terasawa, I., Ikura, T., Gō, N. Structure of melittin bound to perdeuterated dodecylphosphocholine micelles as studied by 2D-NMR and distance geometry calculation. Biochemistry 28:5985–5991, 1989.
11. Braun, W., Gō, N. Calculation of protein conformations by proton-proton distance constrains: a new efficient algorithm. J. Mol. Biol. 186:611–626, 1985.
12. Momany, F. A., McGuire, R. F., Burgess, A. W., Scheraga, H. A. Energy parameters in polypeptides. VII. Geometric parameters, partial atomic charges, nonbonded interactions, hydrogen bond interactions, and intrinsic torsional potentials for the naturally occurring amino acids. J. Phys. Chem. 79:2361–2381, 1975.
13. Némethy, G., Pottle, M. S., Scheraga, H. A. Energy parameters in polypeptides. 9. Updating of geometrical parameters, nonbonded interactions, and hydrogen bond interactions for the naturally occurring amino acids. J. Phys. Chem. 87:1883–1887, 1983.